PHYSICAL REVIEW A **86**, 011602(R) (2012)

Critical rotation of an annular superfluid Bose-Einstein condensate

R. Dubessy, T. Liennard, P. Pedri, and H. Perrin*

Laboratoire de Physique des Lasers, CNRS and Université Paris 13, 99 Avenue J.-B. Clément, F-93430 Villetaneuse, France

(Received 27 April 2012; revised manuscript received 30 May 2012; published 12 July 2012)

We analyze the excitation spectrum of a superfluid Bose-Einstein condensate rotating in a ring trap. We identify two important branches of the spectrum related to outer and inner edge surface modes that lead to the instability of the superfluid. Depending on the initial circulation of the annular condensate, either the outer or the inner modes become first unstable. This instability is crucially related to the superfluid nature of the rotating gas. In particular, we point out the existence of a maximal circulation above which the superflow decays spontaneously, which cannot be explained by invoking the average speed of sound.

DOI: 10.1103/PhysRevA.86.011602 PACS number(s): 03.75.Kk, 47.37.+q

After the pioneering work on persistent flow in helium [1], recent experimental success at producing circulating superfluid flow of Bose gases in annular traps [2–4] has focused interest on the issue of dissipation of this macroscopic quantum state. In a superfluid this question is crucially related to the existence of a critical velocity v_c above which excitations are generated. The critical velocity is determined by the Landau criterion [5]. Dissipation occurs for a fluid velocity larger than v_c. Symmetrically a defect moving above v_c generates excitations in a superfluid at rest. This has been evidenced experimentally in trapped Bose gases [6].

In a homogeneous weakly interacting Bose gas v_c is equal to the speed of sound [7]. This is no longer true if the system is inhomogeneous. For example, in an infinite cylindrically symmetric tube with transverse harmonic confinement, the critical velocity is lower than the speed of sound [8]. In such a geometry, the first modes excited at the critical velocity have been shown to be surface modes [9] propagating along the tube and localized symmetrically all around the edge of the cylinder.

In order to study superfluidity experimentally, it is natural to bind this system and investigate the stability of a persistent flow in a ring geometry. A crucial difference between a tube and a ring is the presence of a centrifugal force arising from the non-Galilean nature of rotation. Moreover, the curvature of the annulus makes the inner and the outer surfaces of the fluid no longer equivalent [10] (see Fig. 1).

The ring geometry has recently attracted a lot of interest. Many annular traps have been proposed [11–13] and realized [2–4,14,15]. Studies of the superfluidity include the observation of a persistent current [2], the effect of a weak link [3,16,17], and the observation of a stepwise dissipation of the circulation [4]. The ground state of the system in the presence of rotation has been determined theoretically [18–20]. Phase fluctuations in a ring trap have also been investigated [21]. However, the determination of the critical angular velocity in a ring is still an open question and is highly relevant to recent experiments [3,4,15].

In this Rapid Communication we determine the critical angular velocity in the sense of the Landau criterion for a Bose gas trapped in a ring. We compute the Bogoliubov excitation spectrum both for an initially nonrotating gas in the ground state, and for an initially circulating stationary state. We show that the critical velocity is governed by surface modes, like in the case of an infinite tube. However, we find that there are now two distinct nondegenerate families of surface excitations propagating either at the inner or at the outer edge. The lowest of these two branches gives the critical angular velocity. Our numerical calculations predict the existence of a maximal circulation, above which the system becomes unstable, any static perturbation giving rise to dissipation of the flow. We give a simple interpretation of all these features by extending the surface mode model [9] to the ring geometry. Our model is in good agreement with the numerical calculations even for an initially circulating state.

We consider a condensate confined in a ring-shaped trap (see Fig. 1) described by the Gross-Pitaevskii equation at zero temperature. For simplicity, we reduce the problem to two dimensions in the plane of the ring. The two-dimensional (2D) ring still allows one to identify the inner and outer edges and evidence their respective roles. The trapping annular potential is written as a harmonic potential of frequency ω_r centered at a radius ρ_0. In the following, we use the associated scales for energy ($\hbar\omega_r$), time (ω_r^{-1}), and length $a_r = \sqrt{\hbar/(M\omega_r)}$, where M is the atomic mass. The 2D Gross-Pitaevskii equation reads

$$i\,\partial_t \psi = \left(-\frac{\Delta}{2} + \frac{1}{2}(r - r_0)^2 + g|\psi|^2\right)\psi, \qquad (1)$$

where $\psi = \psi(r,\theta,t)$ is normalized to unity, $\Delta = \partial_r^2 + \partial_r/r + \partial_\theta^2/r^2$ is the Laplacian in polar coordinates (r,θ), $r_0 = \rho_0/a_r$

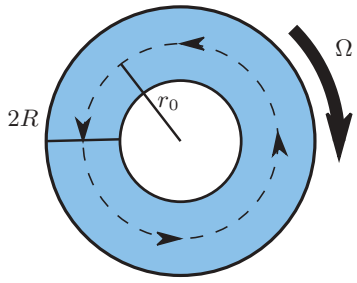

FIG. 1. (Color online) Sketch of the system: A Bose gas flowing with a circulation ℓ (dashed line) and a Thomas-Fermi width $2R$ is held in a ring trap of radius r_0. A defect rotating counterflow at angular velocity Ω above the critical velocity will induce dissipation.

*helene.perrin@univ-paris13.fr

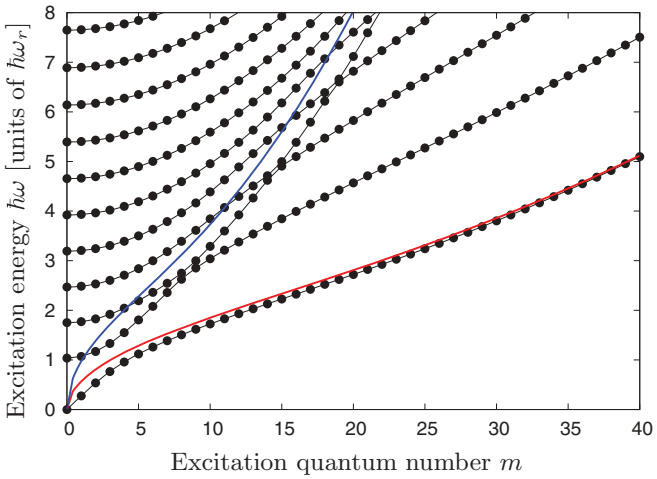

FIG. 2. (Color online) Excitation spectrum obtained from Eq. (1) (see text for details), with $\ell = 0$, $r_0 = 12$, and $g = 9000$. Only the lowest eleven branches are shown. The solid lines are a guide to the eye to distinguish between the different branches. A symmetric spectrum also exists for negative values of m. Solid lines: relation dispersion in the surface mode model for the inner (upper blue line) and outer (lower red line) modes.

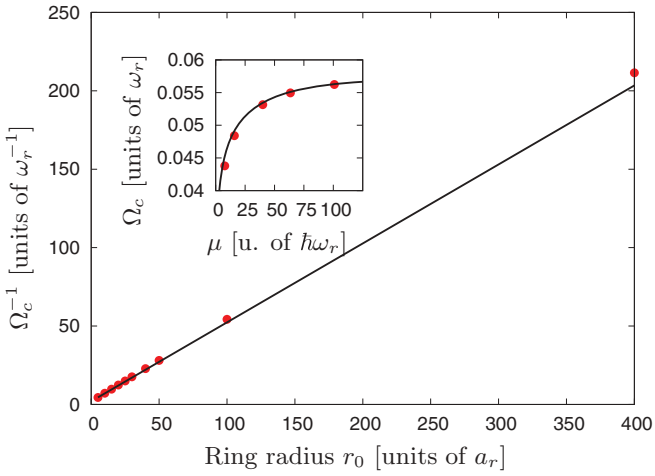

FIG. 3. (Color online) Inverse of the critical angular velocity as a function of the ring radius r_0, at fixed chemical potential [25], as obtained from the full numerical calculation (dots). Inset: critical angular velocity as a function of μ for $r_0 = 40$. In both graphs, the solid line is the model of Eq. (4) with $r_e = r_0 + R$.

is the dimensionless ring radius, and g is the dimensionless interaction constant in two dimensions [22].

Using the rotational invariance of Eq. (1), we consider solutions of the form

$$\psi(r,\theta,t) = e^{-i(\mu t-\ell\theta)}\big[\psi_\ell(r) + \delta\psi_m^\ell(r,\theta,t)\big], \qquad (2)$$

where

$$\delta\psi_m^\ell(r,\theta,t) = u_m^\ell(r)e^{-i(\omega t-m\theta)} + v_m^\ell(r)^* e^{i(\omega^* t-m\theta)}. \qquad (3)$$

The stationary solution $\psi_\ell(r)$ is a state of circulation ℓ and chemical potential μ, which depends on ℓ, and $\delta\psi_m^\ell$ is a small perturbation, parametrized by ℓ and m. $\psi_\ell(r)$ is not necessarily the ground state of the system but can be realized experimentally using phase imprinting [3,4]. We label as $R = \sqrt{2\mu}$ the half width of the radial density distribution in the Thomas-Fermi approximation.

Linearizing Eq. (1), we solve the Bogoliubov–de Gennes equations for $u_m^\ell(r)$ and $v_m^\ell(r)$ [23]. We get real frequencies with a dispersion relation $\omega = \omega_\ell(m)$ for each initial circulation ℓ. The lowest branch of the spectrum allows us to compute the critical angular velocity $\Omega_c(\ell) = \min_m[\omega_\ell(m)/|m|]$ for a given circulation ℓ.

Figure 2 shows a typical spectrum obtained from Eq. (1) for a non-circulating initial state ($\ell = 0$). At small m values, the lowest branch is linear, $\omega_0(m) = m\Omega_s$, and can be associated to rotating soundlike waves with angular velocity Ω_s. At larger m values, this branch exhibits a small negative curvature that makes the critical angular velocity smaller than the angular speed of sound [$\Omega_c(0) < \Omega_s$]. This is not surprising as it is already the case in a linear geometry for an inhomogeneous gas [8,24]. As m increases, the radial profile of the associated density perturbation $\delta\rho_m^0(r)$ of the lowest energy mode, where $\delta\rho_m^\ell(r) = 2\,\mathrm{Re}[\psi_\ell(r)^*(u_m^\ell(r) + v_m^\ell(r)^*)]$, is more and more localized on the outer radius [see Fig. 4(b)]. We thus expect that the mode corresponding to the critical angular velocity will be correctly described by a surface mode model.

Following the approach of Ref. [9], we find the critical velocity for a family of modes lying on the edge of a condensate. Locally, the surface can be considered as a plane, and a surface excitation with wave vector k parallel to this plane gives a critical linear velocity $v_c \simeq \sqrt{2}\mu^{1/6}$ in our dimensionless units, for the critical wave vector $k_c \simeq 0.89 \times \sqrt{2}\mu^{1/6}$ [9]. In our ring-shaped geometry we identify the critical angular velocity as $\Omega_c = v_c/r_e$, where r_e is the radius at which the excitation is localized. Within the surface mode model, the critical angular velocity is then

$$\Omega_c = \frac{\sqrt{2}\mu^{1/6}}{r_e} \qquad (4)$$

and corresponds to a critical excitation $m_c = k_c r_e$, where $r_e \simeq r_0 + R$ (respectively, $r_0 - R$) for an excitation lying on the outer (respectively, inner) edge of the condensate. The dispersion relations of the inner and outer edge surface modes are plotted as solid lines in Fig. 2. For an initial state $\ell = 0$, the inner mode belongs to a higher branch and thus does not determine the critical velocity.

Figure 3 shows a comparison of the full numerical calculation of the critical velocity with the surface mode model. The model of Eq. (4) is in good agreement with the numerical calculation and can thus be used to get an estimation of the critical velocity. We note that the agreement with the numerical calculation is better for larger μ, as shown in the inset of Fig. 3, since the excitation is sufficiently localized on the surface [9].

We now turn to the more complex situation of an initial state with given circulation ℓ, as obtained experimentally in recent experiments [3,4]. Figure 4(a) shows the lower branch of the excitation spectrum for initial states with increasing circulation. As expected, for $\ell > 0$, the spectrum becomes asymmetric, excitations with $m < 0$ propagating against the

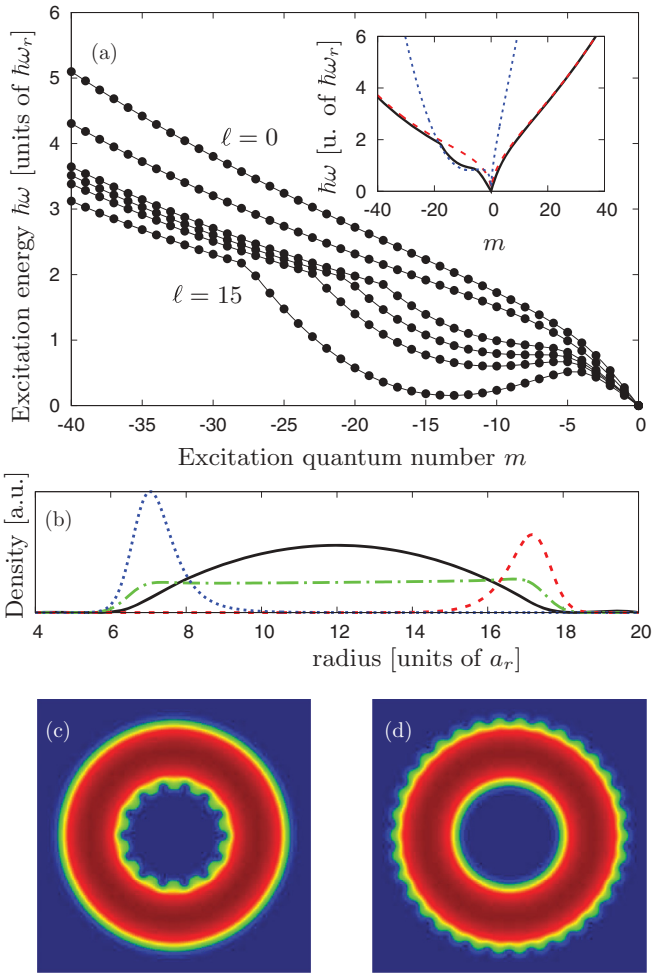

FIG. 4. (Color online) (a) Lower branch of the excitation spectrum for $m < 0$, $r_0 = 12$, $g = 9000$, and initial states with increasing circulation, $\ell = 0,6,11,12,13,15$. Inset: full spectrum for $\ell = 11$ (black solid line) and surface mode model relation dispersion for outer mode (red dashed line) or inner mode (blue dotted line). (b) Radial density profiles of the condensate (black solid line), soundlike mode ($\ell = 0$, $m = -1$, green dash-dotted line, scaled $\times 3$ for clarity), inner edge surface mode ($\ell = 15$, $m = -14$, blue dotted line), and outer edge surface mode ($\ell = 0, m = -34$, red dashed line). (c),(d) Corresponding plot of the atomic density with a population of 10% in the inner mode (c) and the outer mode (d). The size of both images is 40×40 in units of a_r. At the periphery of the gas, 14 vortices appear in (c) and 34 antivortices appear in (d).

superflow having lower energies than those with $m > 0$ [see Fig. 4(a), inset]. One striking feature of this spectrum is that for a sufficiently large ℓ, the critical velocity is associated with a branch that crosses the outer edge surface mode branch. The radial profile $\delta\rho_\ell^m(r)$ shows that these modes are located at the inner edge of the ring [see Fig. 4(b)]. Hence, depending on the initial circulation, the most probable mechanism for dissipation implies either outer or inner modes. Interestingly, the phase profile of the perturbation displays antivortex patterns on the outer edge for outer modes and vortex patterns on the inner edge for inner modes. This supports the idea that these modes are precursors of (anti)vortex nucleation. The total density $|\psi|^2$ with a fraction of 10% in the excited mode is displayed in Fig. 4(c) for the inner mode, and Fig. 4(d) for the outer mode. In both cases, vortices (antivortices) are located on the inner (outer) edge of the gas where the density vanishes.

This result can be understood by extending the surface mode model to an initial state with circulation. It is important to remark that due to the superfluid nature of the condensate flow, the local velocity at the inner edge is larger than the one at the outer edge. In the frame corotating with one of these edges, where the condensate surface is at rest, the result of the surface mode model still holds. In the laboratory frame, the critical angular velocity is then shifted by the angular velocity of the corotating frame: $\Omega_r = \ell/r_e^2$, which depends on the edge considered, and may be written

$$\Omega_c(\ell) = \frac{\sqrt{2}\mu^{1/6}}{r_e} - \frac{\ell}{r_e^2}. \tag{5}$$

The result of Eq. (5) is the sum of two contributions: the first one arises from the surface mode model, whereas the second one is due to the superfluid rotation of the condensate itself. These two terms depend with different power laws on the excited mode radius r_e and this feature explains the transition between inner and outer edge surface excitations observed in Fig. 4(a) (see inset).

Figure 5 shows the critical angular velocity as a function of the initial state circulation ℓ. The curves exhibit a piecewise linear dependence on the circulation. The two slopes correspond, respectively, to modes lying on the outer or inner edge. The critical angular velocity and these slopes are compared to the surface mode model. The agreement is good except for small radii where the centrifugal term $1/r$ in the Laplacian plays an important role, especially in the case of the inner mode. At large values of r_0 the difference between inner and outer modes becomes less pronounced as the system resembles more and more an infinite tube, where these modes are degenerate.

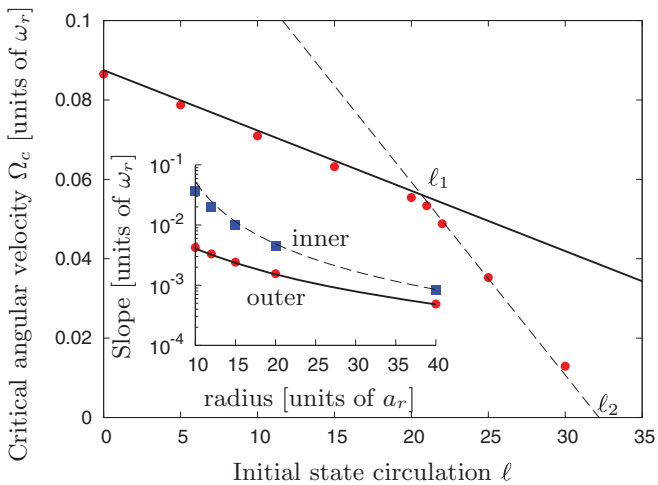

FIG. 5. (Color online) Critical angular velocity versus initial state circulation, as obtained from the numerical solution (dots), for $r_0 = 20$ and $g = 15\,000$. Inset: slope of the critical velocity for inner (blue squares) and outer (red dots) modes versus the ring radius, at fixed chemical potential [25]. For both graphs, the lines are the predictions of Eq. (5), for $r_e = r_0 + R$ (solid line) and $r_e = r_0 - R$ (dashed line).

To interpret the data we define two thresholds. The first threshold $\ell_1 = \mu^{1/6}(r_0^2 - R^2)/(\sqrt{2}r_0)$ is obtained when Eq. (5) gives the same value for $r_e = r_0 \pm R$. It corresponds to the frontier between the domains where either the inner or the outer modes govern dissipation. We find that above a second threshold $\ell_2 = \sqrt{2}\mu^{1/6}(r_0 - R)$, for which the critical angular velocity vanishes, the system is unstable, in the sense that the computed spectra contain negative energies. Any static perturbation of the system thus triggers dissipation and circulation becomes highly unstable. It is important to point out that the value of ℓ_2 is related to the velocity of the surface mode, not to the speed of sound.

From a practical point of view, this sets an upper limit on the circulation that can be imprinted for a given ring radius and chemical potential. Therefore, even if the ring geometry is adapted to study the persistent flow of a superfluid, it can bear only a limited amount of circulation.

Within this model we can make predictions for the superflow stability in recent experiments. In the presence of static defects, the superflow will be unstable for $\ell > \ell_2$. We compute this maximum allowed circulation for a stable flow with the experimental parameters of Ref. [3], namely, $r_0 = 10$ and $\mu = 10.9$, and find $\ell_2 \simeq 11$. We may wonder if our 2D model applies to three-dimensional (3D) experiments. The surface mode model depends only on the force at the surface [9]. For a harmonically trapped BEC, this force is fully determined by the Thomas-Fermi radius and the oscillation frequency. A 2D model is thus expected to compare well to a 3D experiment with the same Thomas-Fermi radius (or chemical potential).

Our results enlighten the recent work of Ref. [16] where a dynamical simulation of a circulating annular Bose-Einstein condensate in the presence of a static weak link shows a dissipation mechanism based on two critical barrier heights, associated to a vortex-antivortex annihilation. Our work shows that indeed a static defect can induce dissipation by first coupling to an inner edge surface mode, allowing a vortex to nucleate, as shown in Fig. 4(c). The excitation of the outer edge surface mode, implying antivortices located all around the outer edge [see Fig. 4(d)], requires a stronger excitation.

In conclusion we have computed the Bogoliubov spectrum of circulating annular Bose gases and obtained analytical expressions for the critical angular velocity based on a surface mode model. We have pointed out the role of inner and outer modes in the determination of the critical angular velocity. We have discussed the implications of these results to explain the dissipation of a persistent flow and have shown that the circulation is unstable above a given threshold. In fact, the Landau argument [5] is quite subtle in a ring geometry. Indeed, as shown in this paper, we find different results for the motion of a defect in a superfluid at rest or for a circulating superfluid flowing through a static defect. In the former case outer edge surface modes are always excited first, while in the latter case the inner edge surface modes dominate. This suggests that in an annular geometry the notion of local speed of sound, associated with modes centered at the peak density, is not the most relevant to discuss superfluidity.

Further work will include a numerical study of the dynamics of an annular Bose gas in the presence of static and rotating defects to further investigate the critical velocity. In particular, we expect that engineering the shape of a perturbation may help to selectively excite only the critical mode and thus more precisely control the system. An interesting point would be to examine the possibility of inducing a circulation by selectively exciting this mode. Symmetrically, while it is clear from our results that dissipation of a flow with an initial circulation $\ell > \ell_2$ first occurs through the appearance of vortices at the inner edge, the subsequent evolution is an interesting open question which will require the simulation of the full dynamics.

ACKNOWLEDGMENTS

Laboratoire de physique des lasers is UMR 7538 of CNRS and Paris 13 University. LPL is part of the Institut Francilien de Recherche sur les Atomes Froids (IFRAF). H.P. acknowledges support from the iXCore Foundation for Research.

[1] H. E. Hall, Philos. Trans. R. Soc. London, Ser. A **250**, 359 (1957).
[2] C. Ryu, M. F. Andersen, P. Cladé, V. Natarajan, K. Helmerson, and W. D. Phillips, Phys. Rev. Lett. **99**, 260401 (2007).
[3] A. Ramanathan, K. C. Wright, S. R. Muniz, M. Zelan, W. T. Hill, C. J. Lobb, K. Helmerson, W. D. Phillips, and G. K. Campbell, Phys. Rev. Lett. **106**, 130401 (2011).
[4] S. Moulder, S. Beattie, R. P. Smith, N. Tammuz, and Z. Hadzibabic, arXiv:1112.0334.
[5] L. D. Landau, J. Phys. (USSR) **5**, 71 (1941).
[6] C. Raman, M. Köhl, R. Onofrio, D. S. Durfee, C. E. Kuklewicz, Z. Hadzibabic, and W. Ketterle, Phys. Rev. Lett. **83**, 2502 (1999).
[7] A. Leggett, Rev. Mod. Phys. **71**, S318 (1999).
[8] P. O. Fedichev and G. V. Shlyapnikov, Phys. Rev. A **63**, 045601 (2001).
[9] J. R. Anglin, Phys. Rev. Lett. **87**, 240401 (2001).
[10] R. Donnelly and A. Fetter, Phys. Rev. Lett. **17**, 747 (1966).
[11] E. M. Wright, J. Arlt, and K. Dholakia, Phys. Rev. A **63**, 013608 (2000).
[12] O. Morizot, Y. Colombe, V. Lorent, H. Perrin, and B. M. Garraway, Phys. Rev. A **74**, 023617 (2006).
[13] I. Lesanovsky and W. von Klitzing, Phys. Rev. Lett. **99**, 083001 (2007).
[14] W. H. Heathcote, E. Nugent, B. T. Sheard, and C. J. Foot, New J. Phys. **10**, 043012 (2008).
[15] B. E. Sherlock, M. Gildemeister, E. Owen, E. Nugent, and C. J. Foot, Phys. Rev. A **83**, 043408 (2011).
[16] F. Piazza, L. A. Collins, and A. Smerzi, Phys. Rev. A **80**, 021601 (2009).
[17] C. Schenke, A. Minguzzi, and F. W. J. Hekking, Phys. Rev. A **84**, 053636 (2011).
[18] A. L. Fetter, Phys. Rev. **153**, 285 (1967).

[19] M. Cozzini, B. Jackson, and S. Stringari, Phys. Rev. A **73**, 013603 (2006).

[20] A. Aftalion and P. Mason, Phys. Rev. A **81**, 023607 (2010).

[21] L. Mathey, A. Ramanathan, K. C. Wright, S. R. Muniz, W. D. Phillips, and C. W. Clark, Phys. Rev. A **82**, 033607 (2010).

[22] $g = N\sqrt{8\pi}\,\frac{a}{a_z}$, where N is the atom number, a is the scattering length, and a_z is the ground-state size along the strongly confined direction z (see, for example, [26]).

[23] The initial stationary state of circulation ℓ is found as the result of an imaginary time propagation of a test Thomas-Fermi profile stopped when the relative variation of the chemical potential reaches 10^{-12}. The Bogoliubov–de Gennes equations are diagonalized using a C++ implementation of the LAPACK library [27].

[24] S. Stringari, Phys. Rev. A **58**, 2385 (1998).

[25] More precisely we keep the ratio g/r_0 constant so that the chemical potential and hence the transverse profile of the condensate are roughly constant. Indeed in the Thomas-Fermi limit μ is expected to scale as $(g/r_0)^{2/3}$ [12].

[26] D. S. Petrov, M. Holzmann, and G. V. Shlyapnikov, Phys. Rev. Lett. **84**, 2551 (2000).

[27] E. Anderson, Z. Bai, C. Bischof, S. Blackford, J. Demmel, J. Dongarra, J. Du Croz, A. GreenBaum, S. Hammarling, A. McKenney, and D. Sorensen, LAPACK *Users' Guide*, 3rd ed. (SIAM, Philadelphia, PA, 1999).